Journal of Sensor Science and Technology
Vol. 22, No. 2 (2013) pp. 100-104
http://dx.doi.org/10.5369/JSST.2013.22.2.100
pISSN 1225-5475/eISSN 2093-7563

Fabrication of a Superhydrophobic Water-Repellent Mesh for Underwater Sensors

Taechang An+

Abstract

A superhydrophobic mesh is a unique structure that blocks water, while allowing gases, sound waves, and energy to pass through the holes in the mesh. This mesh is used in various devices, such as gas- and energy-permeable waterproof membranes for underwater sensors and electronic devices. However, it is difficult to fabricate micro- and nano-structures on three-dimensional surfaces, such as the cylindrical surface of a wire mesh. In this research, we successfully produced a superhydrophobic water-repellent mesh with a high contact angle (>150°) for nanofibrous structures. Conducting polymer (CP) composite nanofibers were evenly coated on a stainless steel mesh surface, to create a superhydrophobic mesh with a pore size of 100 μm. The nanofiber structure could be controlled by the deposition time. As the deposition time increased, a high-density, hierarchical nanofiber structure was deposited on the mesh. The mesh surface was then coated with Teflon, to reduce the surface energy. The fabricated mesh had a static water contact angle of 163°, and a water-pressure resistance of 1.92 kPa.

Keywords : Gas permeable mesh, Superhydrophobic surface, Underwater sensor, Water-repellent mesh

1. INTRODUCTION

Superhydrophobic surfaces with a high water contact angle (WCA) of >150° and a low sliding angle (<10°) provide very attractive functionalities for many applications [1-4], such as self-cleaning, anti-icing, and drag-reduction coatings. The contact angle of the hydrophobic surface depends on the surface chemistry and roughness of the surface. The roughness of a hydrophobic surface enhances its hydrophobicity and stability [1, 5-7].

Carbon nanotubes (CNTs) are attractive for the nanostructure fabrication of superhydrophobic materials [8-11]. However, the substrate material that can be used is limited, due to the high-temperature processing required for CNT growth, such as chemical vapor deposition (CVD) [9]. To solve this problem, CNTs have been immobilized on the surface, using chemical binding and adhesive polymers [10]. However, the surface immobilization technique has several problems, including limited CNT density control, complex chemical treatments, a weak adhesive force, and low stability.

A superhydrophobic mesh is a unique structure that can be used to block water, while allowing energy and gas to pass through holes in the mesh [1, 12]. These meshes have been used in various devices, such as gas- and energy-permeable waterproof membranes for electronic devices [13, 14]. However, it is difficult to fabricate micro- and nano-fibrous structures on a three-dimensional (3D) surface, such as the cylindrical surface of a wire mesh.

In this research, a composite of multi-walled carbon nanotube-polypyrrole (MWNT-PPy) nanofibers was evenly coated on a stainless steel (SS) mesh, using electropolymerization to create a superhydrophobic mesh. PPy acted as a glue to affix the nanofibers to the SS mesh surface, and immobilize them. The nanofiber structure was controlled by the deposition time. As the deposition time increased, a high-density, hierarchical nanofiber structure was deposited. The resulting porous nanofiber structure provided a small water contact area, and air pockets, which created a water-repellent mesh.

2. EXPERIMENTAL

Stainless steel (SS) mesh with a pore size of 100 μm was

Department of Mechanical Design Engineering, Andong National University, Gyeongdong-ro, Andong 760-749, Republic of Korea.
+Corresponding author : tcmerias@andong.ac.kr
(Received : Jan. 28, 2013, Revised : Mar. 13, 2013, Accepted : Mar. 14, 2013)

obtained from HanKook Metal (Korea). The pyrrole monomer (PPy) and sodium dodecyl sulfate (SDS) were obtained from Sigma Aldrich, and HCl (35%) was purchased from Samchun Chemical (Korea). The Teflon solution (Teflon® AF 601S1-100-6) was obtained from Dupont, and fluorocarbon solvent (FC-40) was purchased from 3M. Multi-walled carbon nanotubes (MWNT) with diameters of 10-15 nm and lengths of 5-20 μm, manufactured via CVD, were obtained from Hanwha Nanotech (Korea). All aqueous solutions were prepared with deionized (DI) water (>18 MΩcm).

For preparation of the MWNT suspension, the anionic surfactant SDS was used to disperse the MWNTs, and to induce a negative charge on the MWNT surface. The suspension of MWNTs was prepared by sonicating a mixture of 1mg nanotubes and 100 mL of 0.1 wt% SDS solution for 2-3 h, followed by centrifugation at 3000 rpm for 10 min, to remove the undispersed MWNTs.

MWNT/PPy nanofibrous structures were synthesized on bare SS mesh, via electropolymerization. The SS mesh was cleaned with acetone by sonication, and rinsed with isopropyl alcohol and DI water. For electropolymerization, the SS mesh and Pt electrode were immersed in an aqueous electrolyte solution consisting of 10 mL of MWNT suspension, 1 mL of 0.01 M HCl, and 0.1 mL of PPy monomer. An electrical potential (1-2 V) was applied for 60-300 s between the SS mesh (anode) and a Pt electrode (cathode), using a direct current (DC) power supply (Fig. 1). After MWNT/PPy nanofiber synthesis on the SS mesh surface, the mesh was immersed in DI water for ~1 h, to remove SDS from the surface, and dried under an N2 gas flow.

The as-prepared mesh surfaces were dried at 150°C in a convection oven, to remove water molecules from the surface, and then dipped in a 0.5% Teflon solution, diluted using FC-40, for 10 min. The Teflon coating was then cured in an oven at 200°C for 30 min.

Scanning electron microscopy (SEM) images were obtained by a field-emission (FE)-SEM instrument (SU 6600, Hitachi, Japan). The static WCAs were measured between 5 μL DI water droplets and the nanostructured surface, using a drop-shape analysis system (DSA 100, Kruss, Germany) in the sessile drop mode. Sequential images of water droplet impingement were obtained by a high-speed camera (FASTCAM SA3, Photron, USA).

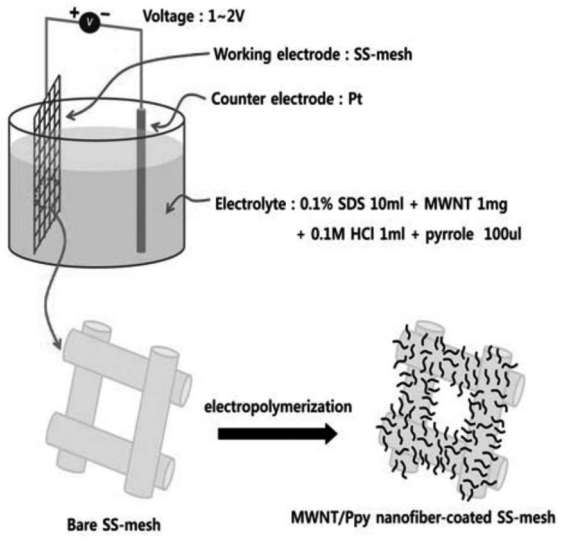

Fig. 1. Schematic diagram of the deposition process of MWNT/PPy nanofibers on the SS mesh surface.

3. RESULTS AND DISCUSSIONS

MWNT/PPy composite nanofibers uniformly coated a bare SS mesh surface by electropolymerization. As the electropolymerization proceeded, the SDS-encapsulated MWNTs moved towards the SS mesh surface, due to the electrostatic interaction between the positive SS mesh surface and the negative SDS molecule of the MWNT surface. MWNT/PPy nanofibers were deposited onto the SS mesh, by polymerization of the pyrrole monomer located at the MWNT surface [15]. Fig. 2 shows SEM images of the rough SS mesh surface, coated with a 3D porous nanostructure composed of MWNT/PPy composite nanofibers. Because MWNTs were used as the template, and PPy acted as the adhesive, MWNT/PPy forest-like nanostructures were created. These structures were firmly attached to the SS mesh, and had a tangled wire configuration that was ~50 nm in diameter (Fig. 2 (b)). The nanofibrous structures increased the surface roughness of the SS mesh, and provided air pockets for the enhanced superhydrophobic mesh. The density of the nanofibers was controlled by the electropolymerization time. As the deposition time increased, the density of the nanofibers increased, and a hierarchical structure was deposited onto the SS mesh surface (Figs. 2 (c) and (d)). The hierarchical surface structure enhanced not only the hydrophobicity, but also the stability of the superhydrophobic surface [1, 16, 17].

We measured the static WCA and water-pressure

resistance of the fabricated hydrophobic mesh. The static WCA of the hydrophobic mesh increased as the surface roughness increased, due to the small water-contact area and air pockets, as shown in Figs. 3 (a) and (b). The static WCA of the smooth-surface Teflon-SS mesh was 148.6 ± 2.8°. However, the Teflon-nanofiber-SS mesh, with a porous nanostructure, had a larger static WCA (163.2 ± 3.4°).

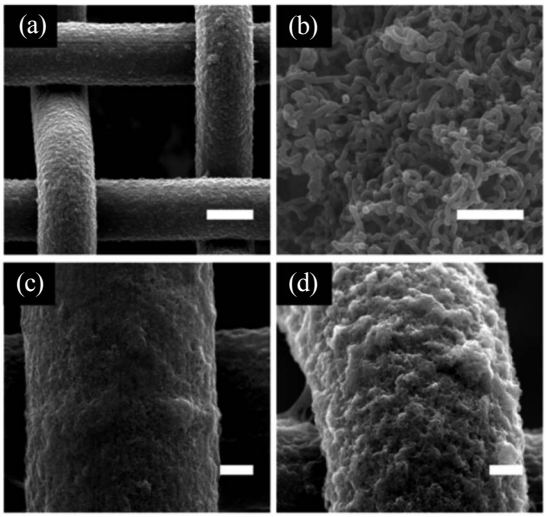

Fig. 2. SEM images of MWNT/PPy nanofiber-coated SS mesh for a magnification of (a) 300× (scale bar: 50 μm) and (b) 20000× (scale bar: 1 μm). SEM images of MWNT/PPy nanofiber-coated SS mesh with different deposition times of (c) 120 s and (d) 300 s (scale bar: 10 μm).

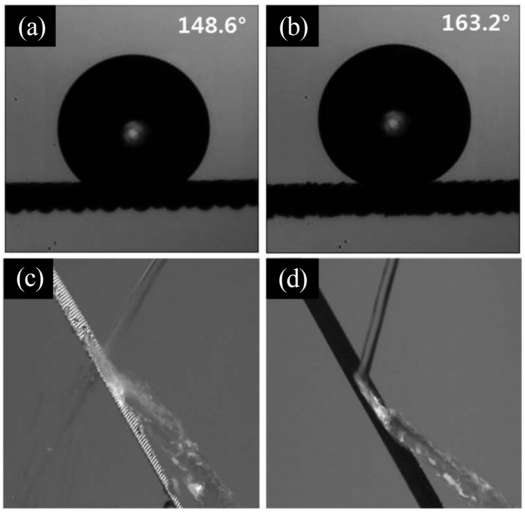

Fig. 3. Static water contact angle (WCA; θ) of (a) Teflon-coated bare SS mesh (Teflon-SS mesh) and (b) Teflon-coated SS mesh with MWNT/PPy nanofibers (Teflon-nanofiber-SS mesh). Photograph of water repellent capabilities of (c) Teflon-SS mesh and (d) Teflon-nanofiber-SS mesh.

Another important property to consider for a superhydrophobic mesh is its water repellent capabilities. To test the water resistance, hydrophobic meshes were secured to the bottom of 6 mm tubes. The inside surfaces of the tubes were coated with Teflon, to minimize the capillary force effect. The vertically standing tubes were then slowly filled with water. The maximum height of the water attained before water leakage through the mesh bottom was determined (Table 1). The maximum water-pressure resistance of the Teflon-SS mesh and Teflon-nanofiber-SS mesh was 1.47±0.07 kPa and 1.92±0.11 kPa, respectively. Figs. 3 (c) and (d) show the difference in the water repellent capabilities between the Teflon-SS mesh and the Teflon-nanofiber-SS mesh. The Teflon-nanofiber-SS mesh, with its superhydrophobic surface, completely repelled the water jet. However, the same water jet partially passed through the Teflon-SS mesh holes. Here, the theoretical maximum water-pressure resistance of the hydrophobic mesh can be explained by the capillary phenomena [18]. Because each hole of the mesh can be considered to be a capillary, the maximum water height can be calculated as follows:

$$h = -\frac{2r\cos\theta}{pgd} \tag{1}$$

where, h, γ, θ, p, and d represent the maximum water height, the surface tension of water, the static contact angle, the density of water, and the effective mesh hole size, respectively. In the case of a square mesh hole, the effective mesh hole size (D) was assumed to be half the width [19]. Theoretical values were obtained from Eq. (1) with the measured static WCA, shown in Table 1. Because the maximum water height is proportional to cos θ, the Teflon-nanofiber-SS mesh had a larger water-pressure resistance than the Teflon-SS mesh. Thus, the measured values were smaller than the theoretical values; this was attributed to the effective mesh hole size measurement (D), and the static WCA (θ). The actual value of the effective mesh hole size was larger than the value we set. Additionally, the static WCA could be decreased by the water pressure [5]. Superhydrophobic surfaces often lose their hydrophobicity under dynamic conditions. We observed that the properties of the hydrophobic surface were highly dependent on the surface roughness (Table 1). The ratio of the measured value and theoretical value of the Teflon-nanofiber-SS mesh was higher than that of the Teflon-SS mesh, because the porous structure of the

nanofiber structure increased its hydrophobicity stability.

Table 1. Comparison of theoretical and measured water-pressure resistance of the hydrophobic mesh

Mesh Type	Maximum water-pressure resistance		$R_M / R_T \times 100$ (%)
	Theoretical value (R_T)	Measured value (R_M)	
Teflon-SS -mesh	2.49 kPa	1.47 ± 0.07 kPa	59%
Teflon-nanofiber-SS-mesh	2.81 kPa	1.92 ± 0.11 kPa	68%

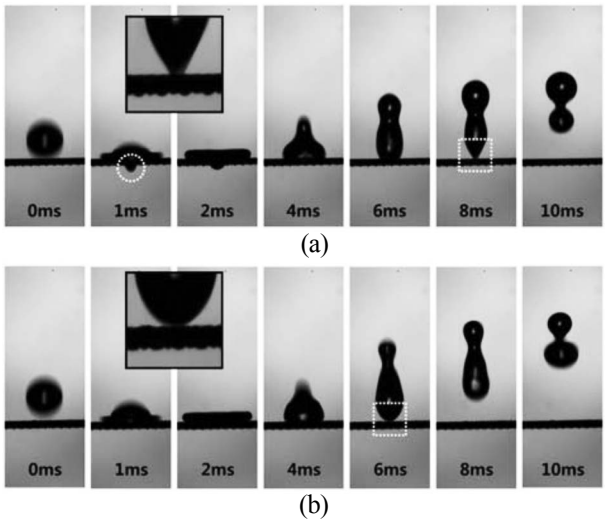

Fig. 4. Sequential images of water droplet impingement on the hydrophobic (a) Teflon-SS mesh and (b) Teflon-nanofiber-SS mesh. The inset shows a magnified image of water droplets bouncing off of the hydrophobic mesh surface.

Finally, we measured the impact behavior of water droplets on the hydrophobic mesh, using a high-speed camera to compare the solid-liquid interactions of hydrophobic surfaces. The chemical properties and structure of the hydrophobic surface affected the solid-liquid interaction [20]. Fig. 4 shows sequential images of water droplet impingement. Free-falling water droplets, with a volume of 10 μL, struck the hydrophobic mesh surface from a height of 6 cm. For the Teflon-SS mesh, some of the droplets bounced off of the surface, while others protruded through the opposite side of the mesh at a pressure (~0.6 kPa) lower than the maximum static water-pressure resistance (~1.47 kPa) (circle area in Fig. 4 (a)). In contrast, the water droplets clearly bounced off of the Teflon-nanofiber-SS mesh, without any leakage through the mesh (Fig. 4 (b)), thus demonstrating the super-hydrophobicity of the surface.

4. CONCLUSIONS

In summary, we successfully fabricated a porous and MWNT/PPy nanofibrous structure on a SS mesh surface, using electropolymerization. The nanofibers uniformly coated and adhered to the 3D cylindrical surface of the mesh. Our fabrication method can be applied to the deposition of nanostructures on various 3D surfaces. After Teflon coating, the nanostructured mesh had better superhydrophobicity, exhibiting a larger static WCA and higher water-pressure resistance, than a mesh with a smooth surface. This enhanced hydrophobicity was attributed to the nanofibrous structure of the mesh surface, which provided small water contact areas and stable air pockets.

ACKNOWLEDGMENT

This work was supported by a grant from the 2012 Research Fund of Andong National University.

REFERENCES

[1] T. C. An, S. J. Cho, W. S. Choi, J. H. Kim, S. T. Lim, and G. B. Lim, "Preparation of stable superhydrophobic mesh with a biomimetic hierarchical structure", *Soft Matter.*, Vol. 7, pp. 9867-9870, 2011.

[2] S. J. Cho, T. C. An, J. Y. Kim, J. W. Sung, and G. B. Lim, "Superhydrophobic nanostructured silicon surfaces with controllable broadband reflectance", *Chem. Commun*., Vol. 47, pp. 6108-6110, 2011.

[3] K. Liu, X. Yao, and L. Jiang, "Recent developments in bio-inspired special wettability", *Chem. Soc. Rev*., Vol. 39, pp. 3240-3255, 2010.

[4] T. Darmanin, E. T. de Givenchy, S. Amigoni, and F. Guittard, "Superhydrophobic surfaces by electro-chemical processes", *Adv. Mater*., Vol. 25, pp. 1378-1394, 2013.

[5] A. Lafuma and D. Quéré, "Superhydrophobic states", *Nat. Mater*., Vol. 2, pp. 457-460, 2003.

[6] X. Yao, L. Xu, and L. Jiang, "Fabrication and characterization of superhydrophobic surfaces with

dynamic stability", *Adv. Funct. Mater*., Vol. 20, pp. 3343-3349, 2010.

[7] K. Acatay, E. Simsek, C. Ow-Yang, and Y. Z. Menceloglu, "Tunable, superhydrophobically stable polymeric surfaces by electrospinning", *Angew. Chem. -Int. Edit.*, Vol. 43, pp. 5210-5213, 2004.

[8] C. H. Lee, N. Johnson, J. Drelich, and Y. K. Yap, "The performance of superhydrophobic and superoleophilic carbon nanotube meshes in water-oil filtration", *Carbon*, Vol. 49, pp. 669-676, 2011.

[9] C. S. Lee and S. H. Baik, "Vertically-aligned carbon nano-tube membrane filters with superhydrophobicity and superoleophilicity", *Carbon*, Vol. 48, pp. 2192-2197, 2010.

[10] Y. Liu, J. Tang, R. Wang, H. Lu, L. Li, Y. Kong, K. Qi, and J. H. Xin, "Artificial lotus leaf structures from assembling carbon nanotubes and their applications in hydrophobic textiles", *J. Mater. Chem*., Vol. 17, pp. 1071-1078, 2007.

[11] G. Li, H. Wang, H. Zheng, and R. Bai, "A facile approach for the fabrication of highly stable superhydrophobic cotton fabric with multi-walled carbon nanotubes-azide polymer composites", *Langmuir*, Vol. 26, pp. 7529-7534, 2010.

[12] D. Tian, X. Zhang, J. Zhai, and L. Jiang, "Photocontrollable water permeation on the micro/nanoscale hierarchical structured ZnO mesh films", *Langmuir*, Vol. 27, pp. 4265-4270, 2011.

[13] S. J. Lee, S. T. Kim, and H. S. Kim, "A study on the measurement of halitosis of human mouth with chemical gas sensor arrays", *J. Sensor Sci. & Tech*., Vol. 20, pp. 279-285, 2011.

[14] Y. W. Park, H. Y. Shin, and S. J. Yoon, "3-dimensional nanostructured ZnO gas sensor", *J. Sensor Sci. & Tech*., Vol. 19, pp. 356-360, 2010.

[15] X. Zhang, J. Zhang, and Z. Liu, "Conducting polymer/carbon nanotube composite films made by in situ electropolymerization using an ionic surfactant as the supporting electrolyte", *Carbon*, Vol. 43, pp. 2186-2191, 2005.

[16] Y. Su, B. Ji, K. Zhang, H. Gao, Y. Huang, and K. Hwang, "Nano to micro structural hierarchy is crucial for stable superhydrophobic and water-repellent surfaces", *Langmuir*, Vol. 26, pp. 4984-4989, 2010.

[17] N. Michael and B. Bhushan, "Hierarchical roughness makes superhydrophobic states stable", *Micro-electron. Eng*., Vol. 84, pp. 382-386, 2007.

[18] Z. X. Jiang, L. Geng, and Y. D. Huang, "Design and fabrication of hydrophobic copper mesh with striking loading capacity and pressure resistance", *J. Phys. Chem*. C, Vol. 114, pp. 9370-9378, 2010.

[19] N. Ichikawa, K. Hosokawa, and R. Maeda, "Interface motion of capillary-driven flow in rectangular microchannel", *J. Colloid Interface Sci*., Vol. 280, pp. 155-164, 2004.

[20] P. Tsai, S. Pacheco, C. Pirat, L. Lefferts, and D. Lohse, "Drop impact upon micro- and nanostructured superhydrophobic surfaces", *Langmuir*, Vol. 25, pp. 12293-12298, 2009.